Luminosity function of GRBs

RANGEL LEMOS, Luis Juracy

Pos-doc of the
ITA - Instituto Tecnológico de Aeronáutica
This work was developed during my PhD in the La Sapienza University/ICRANet

Guarujá, December 15, 2012

1. History, Fireball model and Compton telescope
2. Fireshell model
3. Luminosity function of GRBs
4. LF statistics applied in GRB data

Introduction and motivation

- We applied the LF statistic in three GRB classes predicted by the Fireshell model (*long*, *genuine short* and *disguised short*).
- To transform useful the data obtained by the old detector BATSE, where they do not have redshift.
- We estimate the number of unobservable sources (effects of the Malmquist bias).
- We explore a possible GRB intrinsic property (L_{iso} vs E_{pk}) that would make the GRBs a standard candle.

GRB Historic highlights - 1

- '60 - Instead of measure nuclear test of USSR, the Vela detector observed γ-rays sources (GRBs) external to the Solar system.
- 1992 - The discoveries of BATSE detector showed that the GRBs are distributed homogeneously, consequently they must be extra-galactic sources. It was also proposed two GRB classes: *short* and *long*.
- 1993 - The GRB spectra were fitted phenomenologically with good accuracy (1993ApJ...413..281Band).
- 1997 - The GRB 970228 was (by Beppo-SAX and Keck) the first source with measured redshift (1997Natur.387..783Costa).

GRB Historic highlights - 2

- 2004 - It was launched the Swift satellite, equipped with three detectors [in optic (UVOP), X-ray (XRT) and γ-ray (BAT)] that improved enormously our knowledge about the GRBs; with high time duration and spectral resolution.
- 2008 - It was launched the Fermi satellite, equipped with two detectors [in soft and hard γ-rays, respectively, GBM and LAT], where, in addition to the high time and spectral resolution, the LAT instrument shows us the extreme high γ-ray emission of the GRBs.
- 2008 - GBM and LAT recorded the most energetic source (GRB 080916C), $E_{iso} = 8.8 \times 10^{54}$ ergs $= 4.9\, M_{\odot}$.
- 2009 - Swift measured the most distant source (GRB 090423), with redshift 8.26.

Fireball model

This model (2005RvMP...76.1143Piran and 2006RPPh...69.2259Mészáros) is the most quoted by the GRB community to explain the physical process of the GRB. They argue that the prompt emission is explained by internal shock of relativistic $e^+ - e^-$ shells with different Lorentz γ-factors; and the afterglow emission is explained by a external shock of a relativistic baryonic-$e^+ - e^-$ shell against the circumburst medium (CBM).

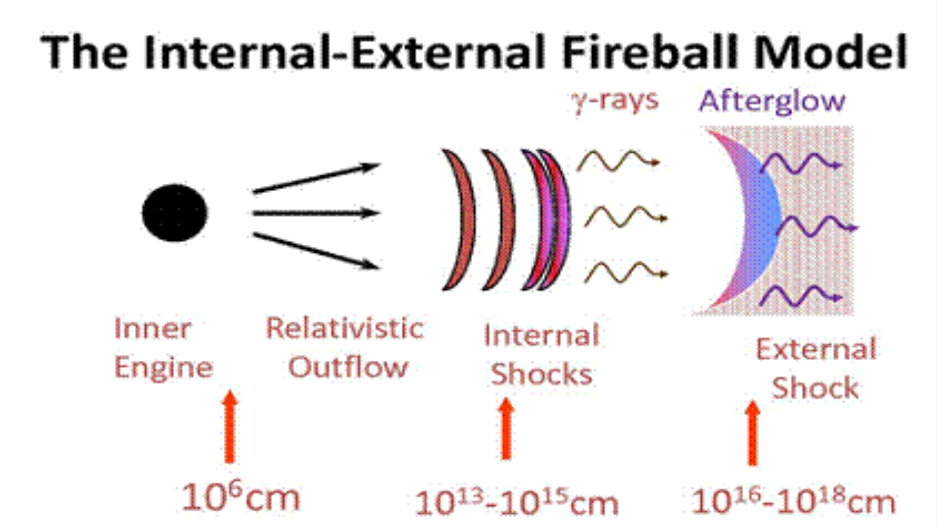

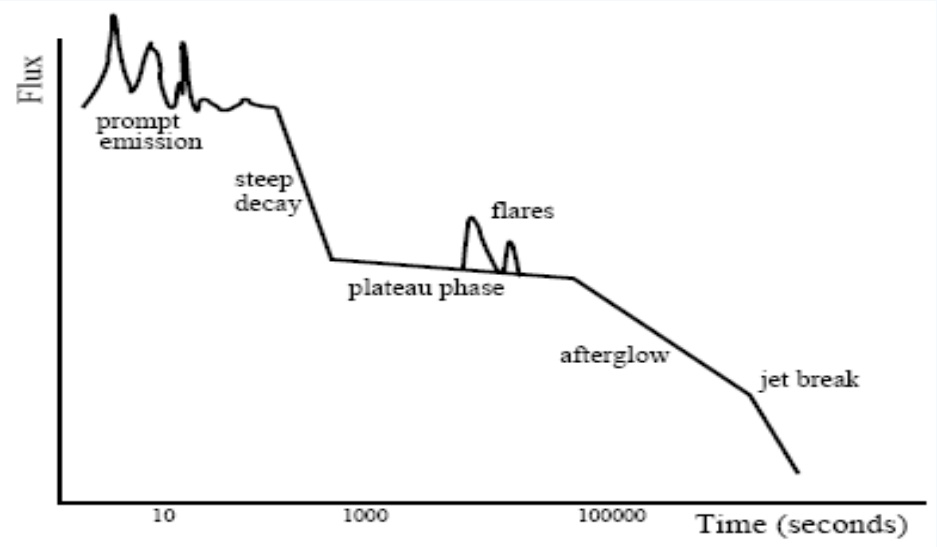

The Fireball model defends that the GRB spectrum is produced by synchrotron processes, where the radiation is produced in the interaction between the positrons and electrons of the relativistic shells and the self magnetic field of the shell. The scheme in the right side illustrate this.

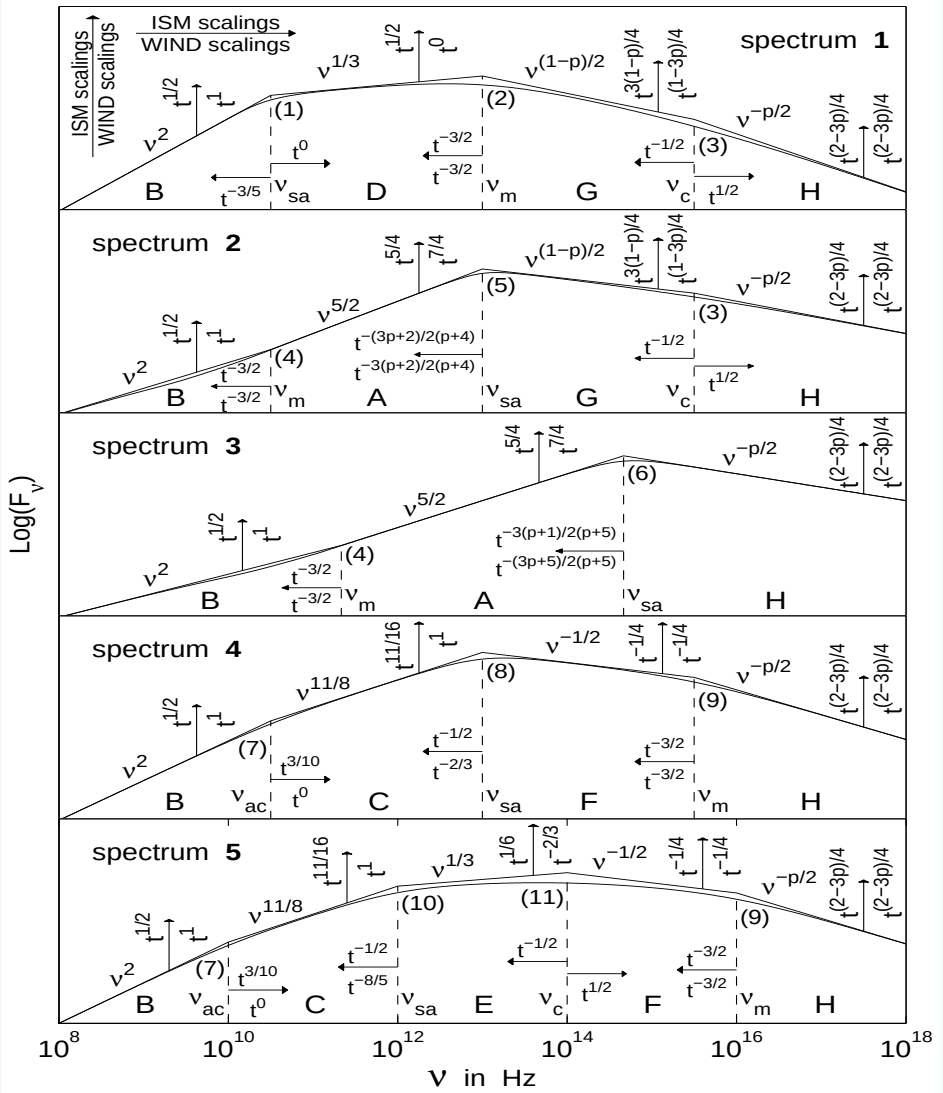

Compton telescope

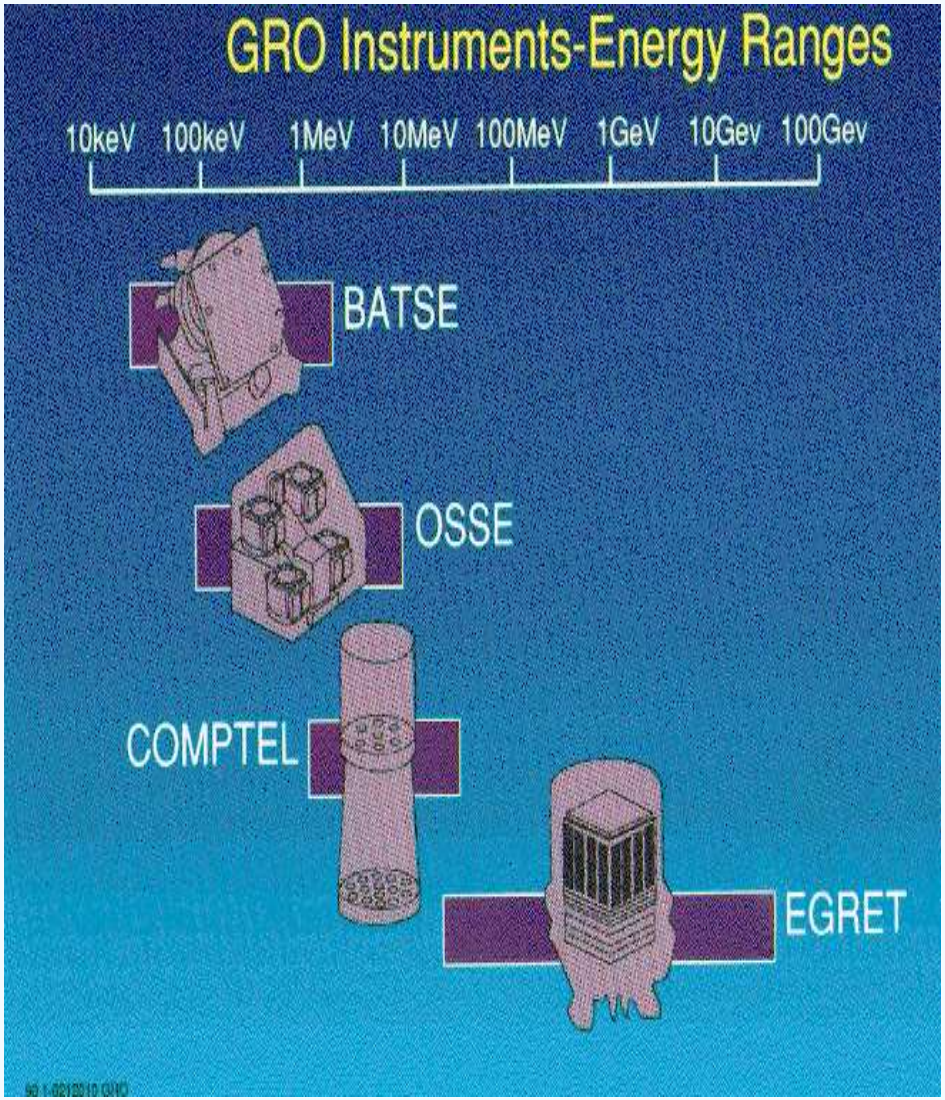

BATSE detector

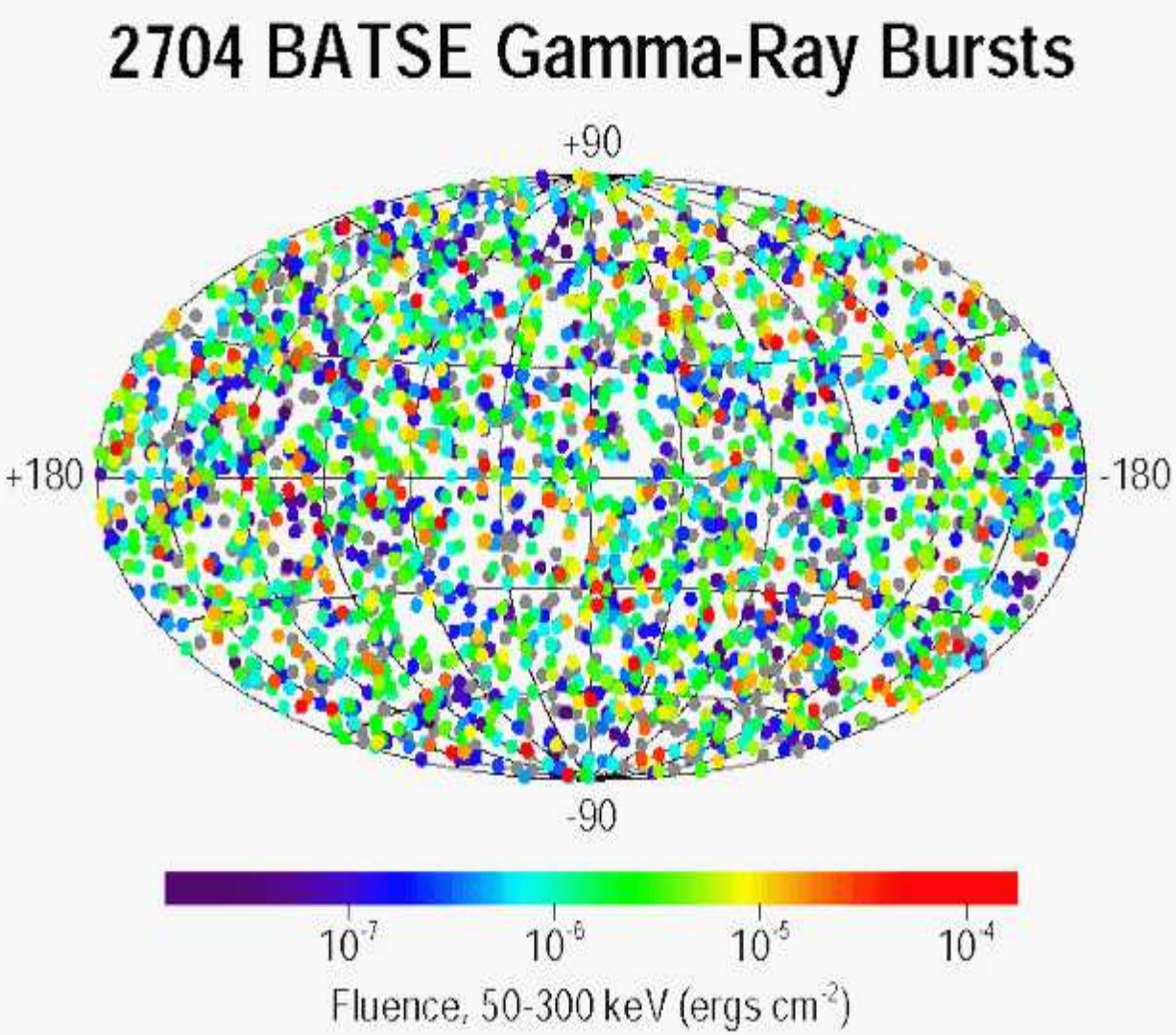

The BATSE instrument measured almost one GRB/day, and from its observations, it was discovered that the GRBs are distributed homogeneously on the sky.

Fireshell model - Interaction with CBM

The Fireshell model claims that all the energy emitted (in all frequencies) after the transparency (P-GRB) is produced by the interaction between the optically thin fireshell and the CBM (2004ApJ...605L...1Bianco), this emission is called *extended afterglow*.

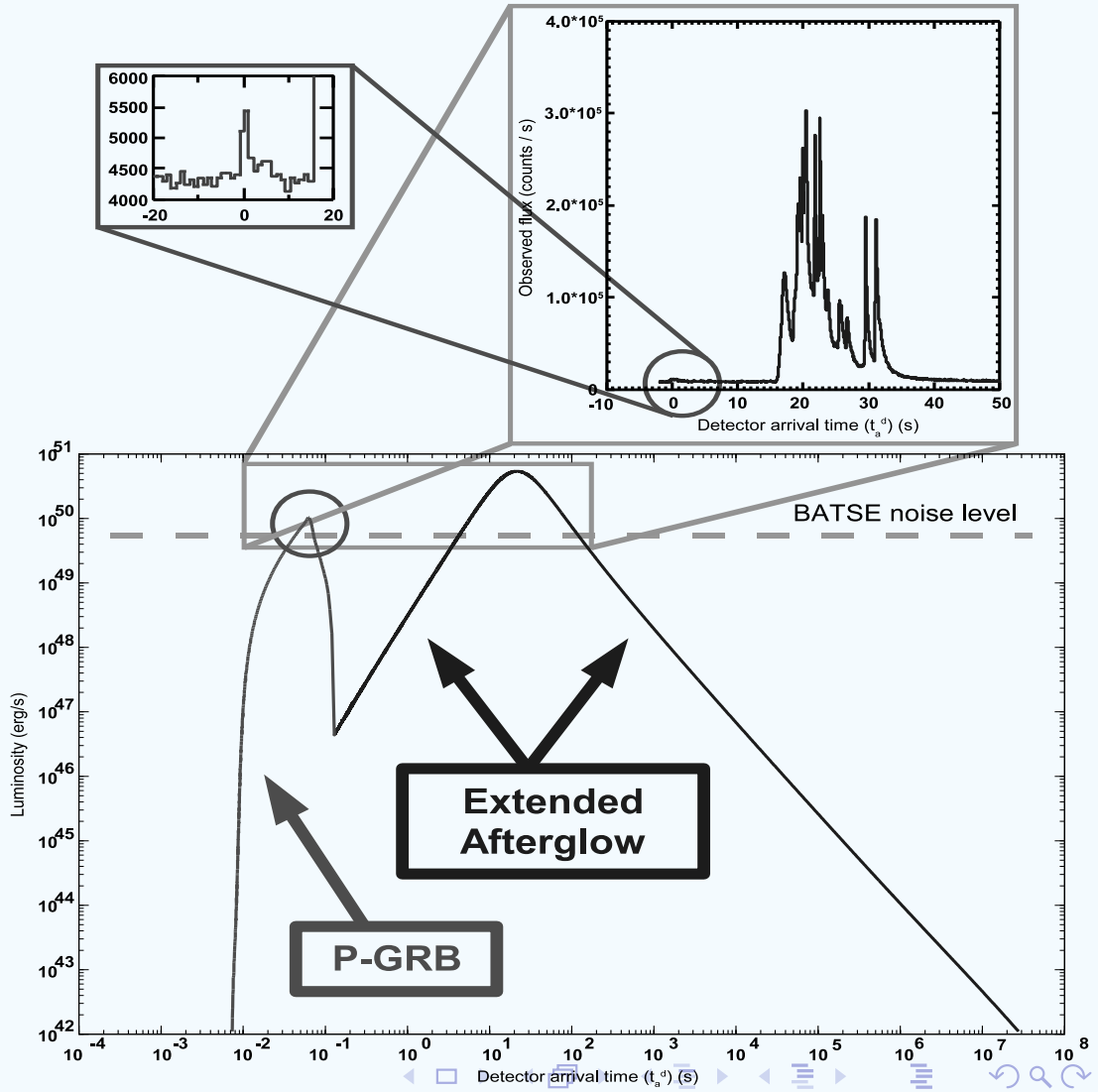

Fireshell model - Genuine short GRB

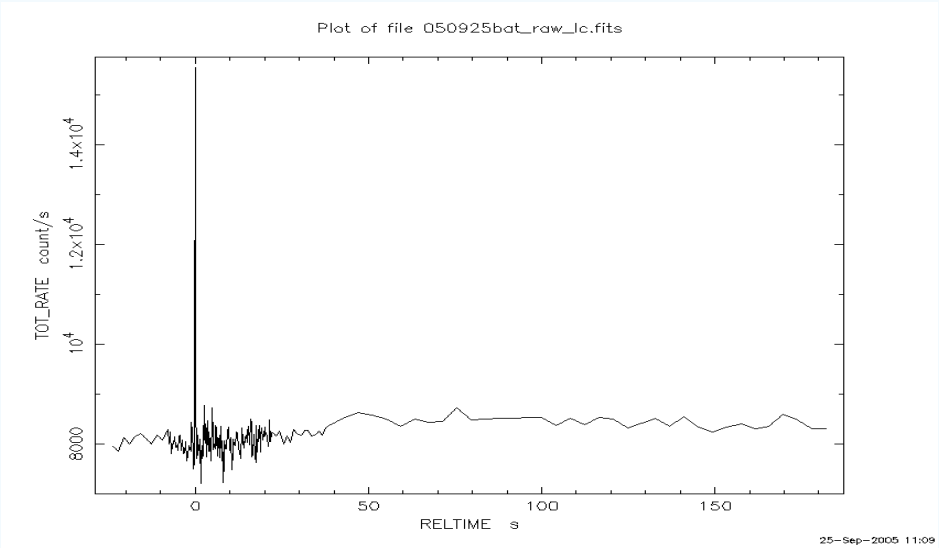

They are the sources in which most of the fireshell energy (equal E_{iso}) is emitted in the transparency (P-GRB emission). These sources are characterized by the difficulties to observe their very weak *extended afterglow*.

Long GRB

In this case, most part of the isotropic energy E_{iso} is emitted in the *extended afterglow*, instead of the P-GRB. The flairs are produced due to the interaction (of the optically thin fireshell) with blobs with high particle density.

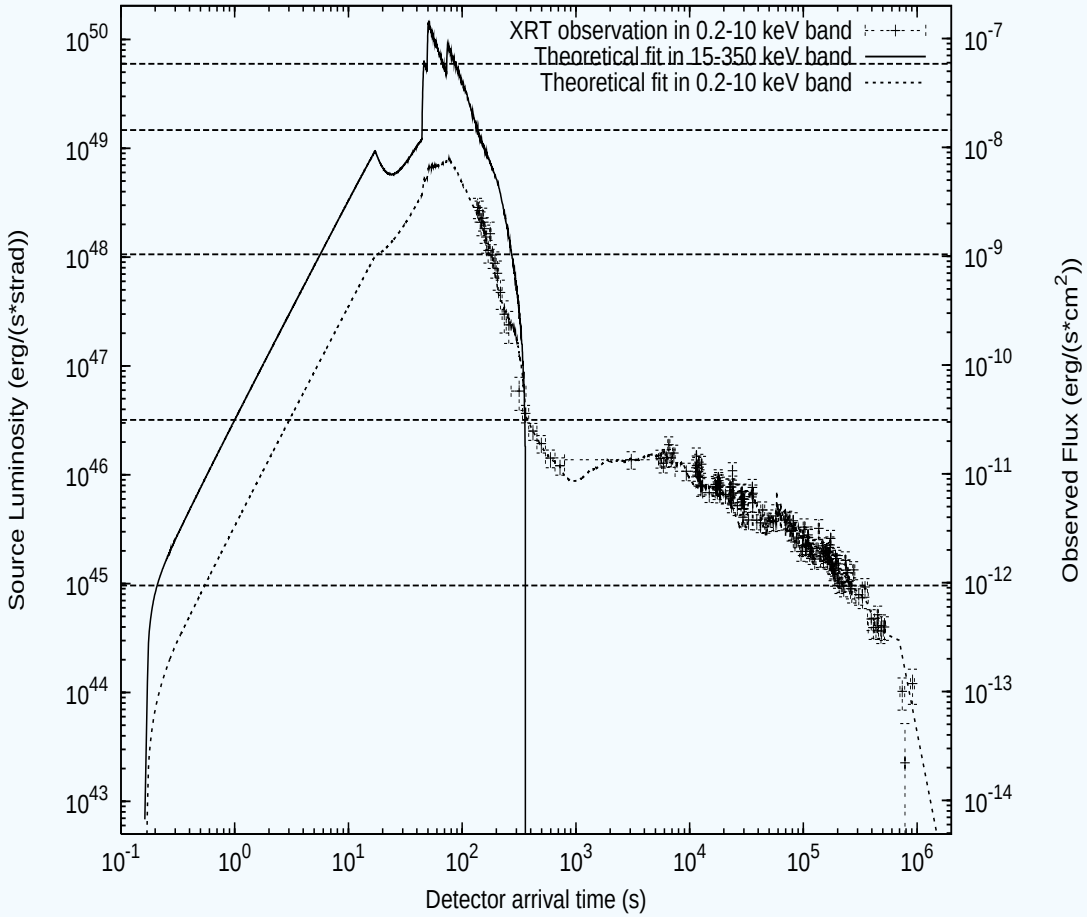

Disguised short GRB

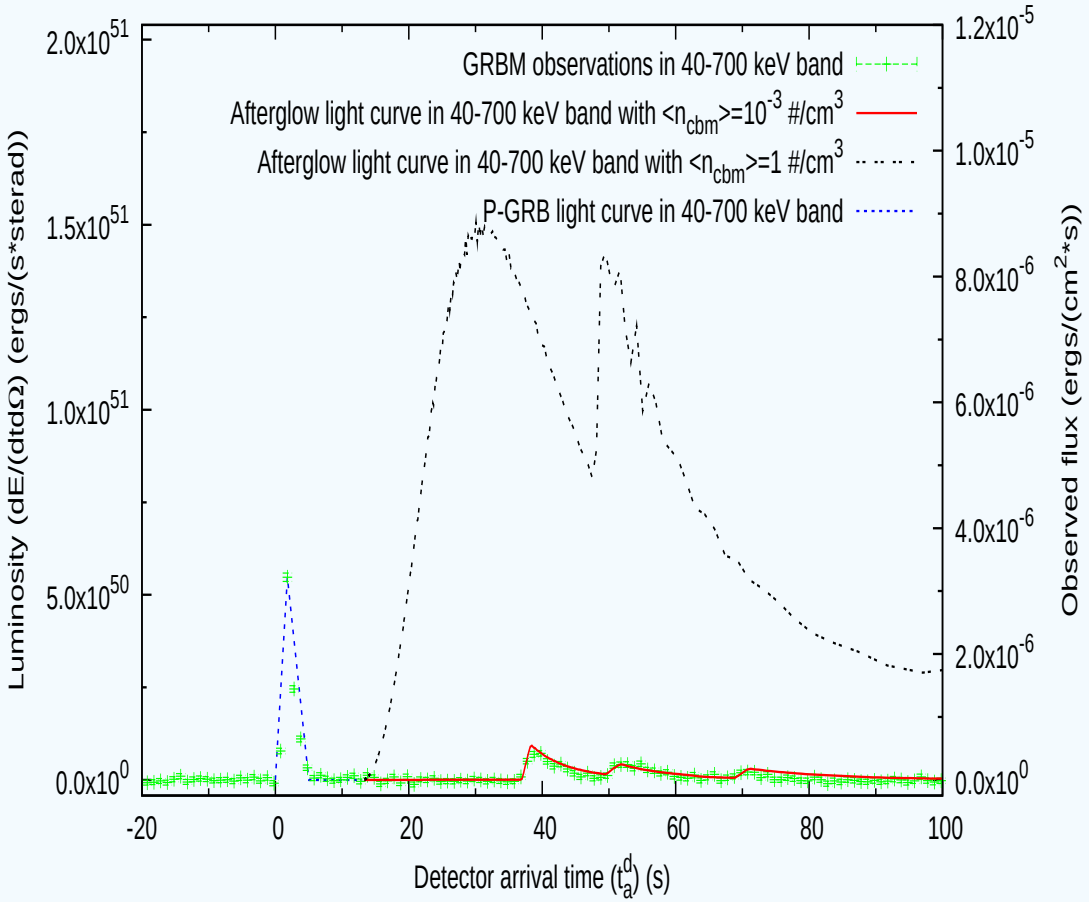

They occur when the CBM density is very low, $\sim 10^{-3} - 10^{-4}$ particles/cm^3 (2007A&A...474L..13B).

Luminosity function of GRBs

Here we perform a review of the works of Maarten Schmidt about the application of the luminosity function statistics in data of BATSE detector. He used the Euclidean value of $\langle V/V_{max} \rangle$ and made a careful analysis of the sensitivity of BATSE detector.

The luminosity function (LF) of a sample of astronomical sources is one of the strongest statistical tools an astrophysics. If we obtain it we can extract several physical information about the sample, but the main difficulty is to yield the intrinsic LF that represents well the sample.

$$\text{Luminosity Function } \Phi(\mathrm{L},\mathrm{R}) \Rightarrow \frac{\text{number of sources}}{[\text{luminosity}]\,[\text{volume}]},$$

$$\text{Source Count } \mathrm{N} = \int \Phi(\mathrm{L},\mathrm{R})\mathrm{dLdV} \Rightarrow \int \Phi(\mathrm{L},\mathrm{z})\mathrm{dLdz}.$$

Euclidean value of V/V_{max}

The V/V_{max} is the ratio between volumes, where V is the volume of the sphere whose radius is the distance between the source and us (D_{source}); and V_{max} is the one whose the radius is the maximal observable distance (D_{max}).

$$\frac{V}{V_{max}} = \left(\frac{D_{source}}{D_{max}}\right)^3 = \left(\frac{F}{F_{lim}}\right)^{-3/2}, \quad (1)$$

where F and F_{lim} are the fluxes associated to the distances, respectively, D_{source} and D_{max}.
The $\langle V/V_{max}\rangle$ is a possible distance indicator, and it was initially used to measure the degree of homogeneity of the radio source distribution in the line-of-sight.

BD1 sample, 1422 GRBs

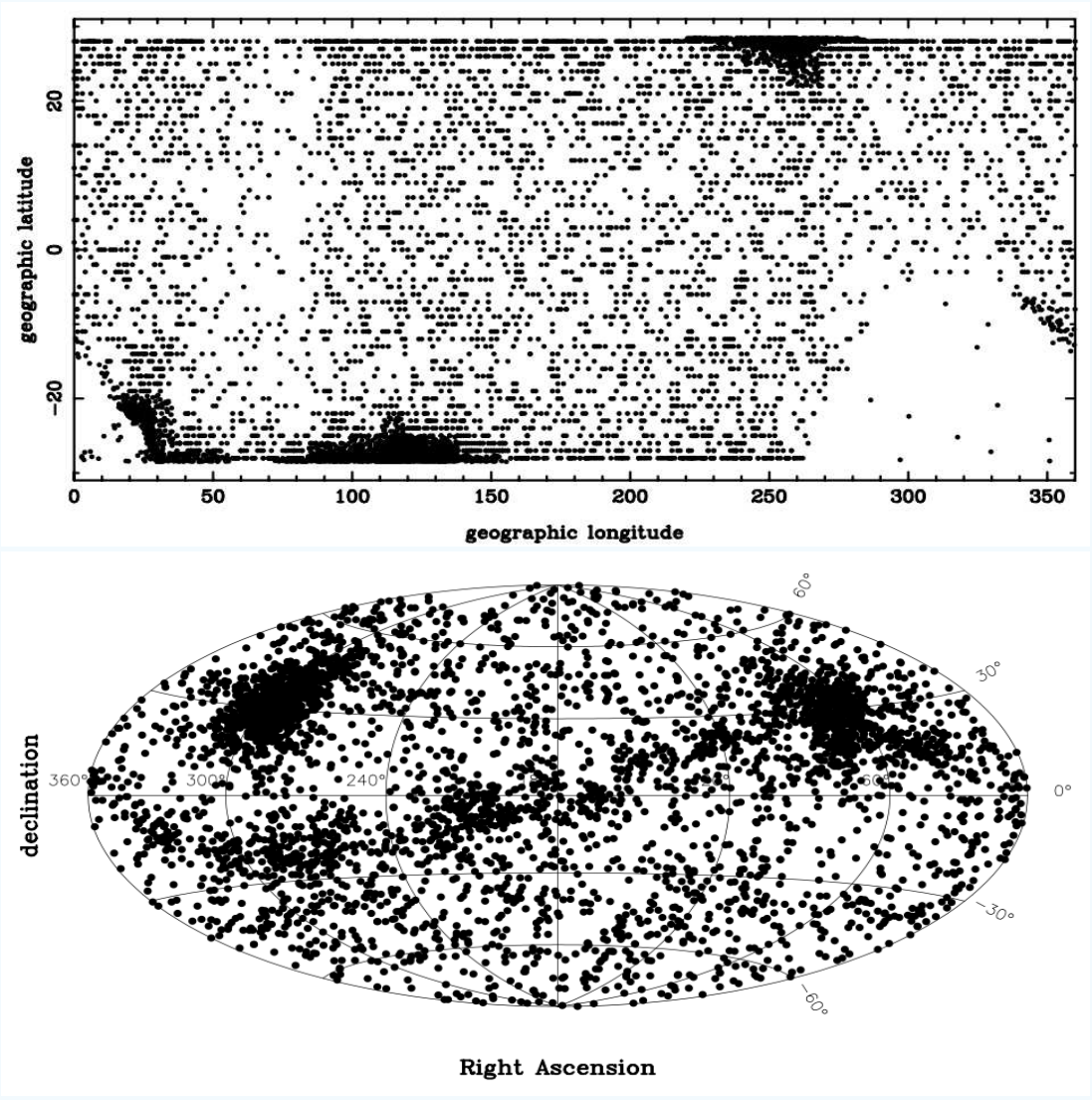

Schmidt (1999A&AS..138..409Schmidt) took 7536 events of 6.2 years of BATSE observation; he eliminated 3051 atmospheric events and 3063 events from the sun and inner Milky Way, leaving 1422 possibles GRBs.

GUSBAD catalog, 2207 GRBs, 9.2 years of observation

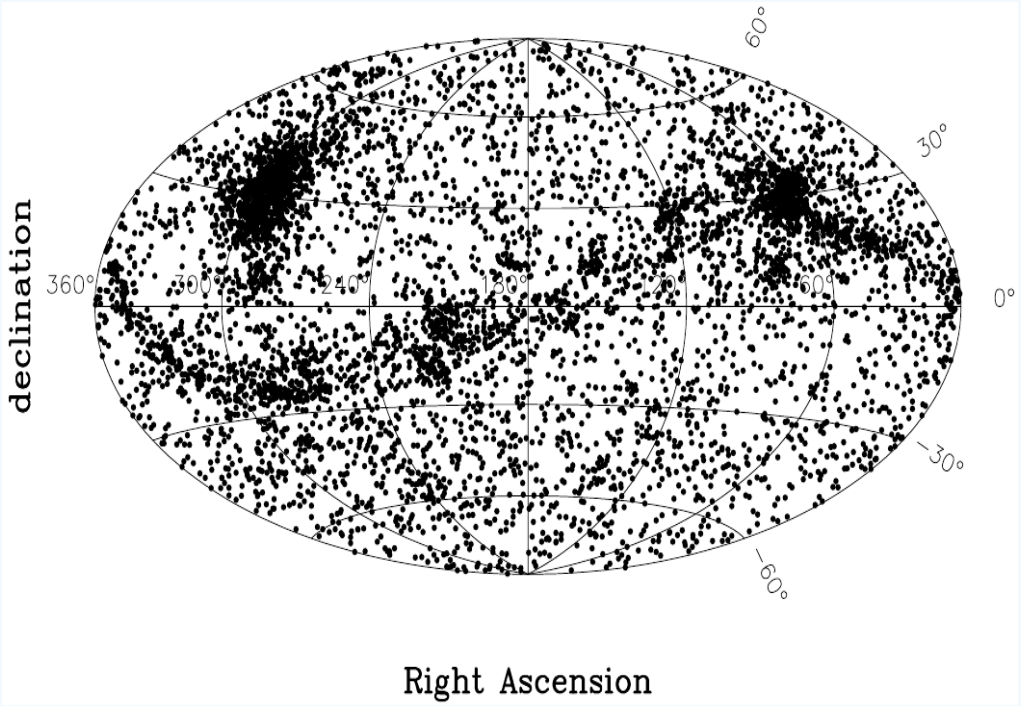

The equatorial coordinates of 6236 events are shown in figure above, we can see the events from three galactic sources: solar flares (along the ecliptic), Nova Persei 1992 (blob in right) and Cygnus region (blob in left).

Luminosity criteria to obtain luminosity function

The LF models can be calibrated according to three luminosity criteria: *variability*, *spectral lag* and *spectral hardness*.

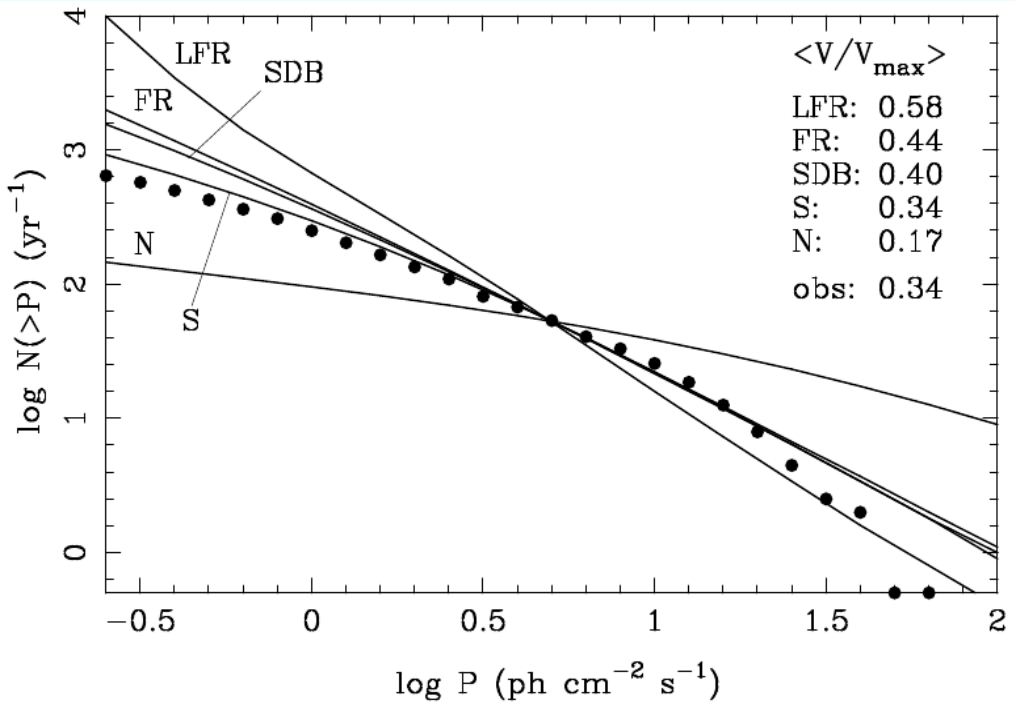

Luminosity function and source count

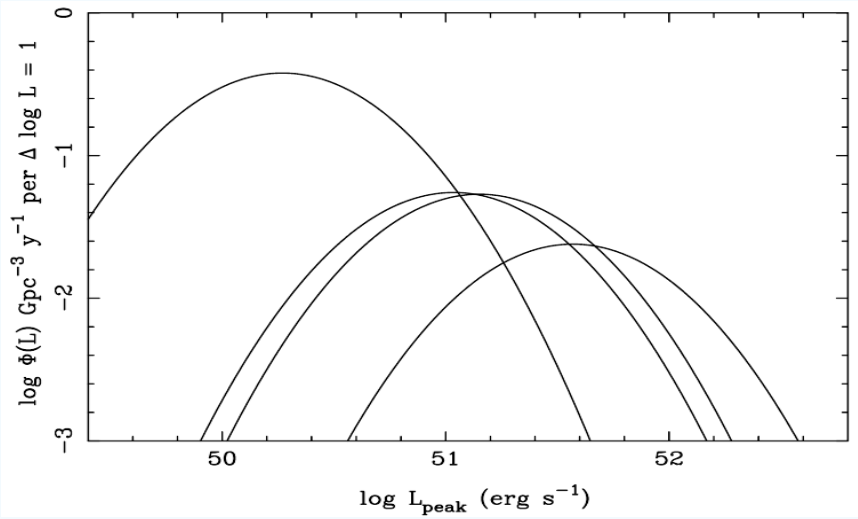

The figures in left side show the Gaussian luminosity functions proposed by Schmidt (2001ApJ...552...36S); and below it is illustrated the peak flux distribution obtained from the observations (dots) and LF prediction (lines) for three GRB rate density models.

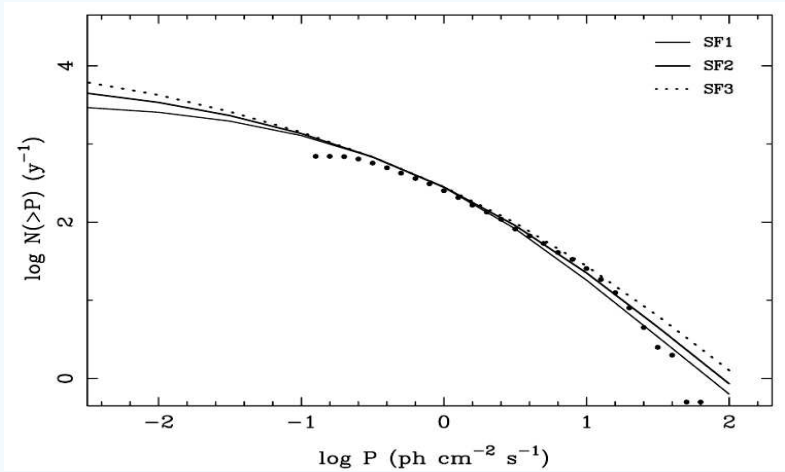

LF statistics applied in GRB classes

Here we apply the LF statistic in three GRB classes predicted by *Fireshell model* (*genuine short*, *disguised short* and *long*). The main goal of this application is to test this prediction using the LF statistic. In doing so, we will proceed: a) to compare the distributions (peak flux, redshift and peak luminosity) for four subsamples of BATSE sources (*total*, *long*, *genuine short* and *disguised short*), b) to estimate the number of unobservable sources (effects of the Malmquist bias), and c) to explore a possible GRB intrinsic property that would make the GRBs a standard candle.

Selections

We identify the *disguised short* by choosing the sources which fulfill the following two conditions

$$\frac{T_{pk}}{T_{tot}} < 0.1, \qquad \text{and} \qquad \mathrm{T_{pk}} < 5 \qquad \text{seconds}, \tag{2}$$

where T_{pk} is the peak time of the light curve measured from the trigger time; and T_{tot} is the total duration of the light curve.

		total		genuine short		long		disguised short	
ch	E^i_{pk}	N_{grb}	$\langle V/V_{max}\rangle$	N_{grb}	$\langle V/V_{max}\rangle$	N_{grb}	$\langle V/V_{max}\rangle$	N_{grb}	$\langle V/V_{max}\rangle$
1	30	24	$0.43_{\pm 0.12}$	7	$0.327_{\pm 0.093}$	13	$0.466_{\pm 0.078}$	3	$0.68_{\pm 0.28}$
2	70	204	$0.463_{\pm 0.034}$	51	$0.436_{\pm 0.036}$	150	$0.455_{\pm 0.024}$	9	$0.455_{\pm 0.093}$
3	185	608	$0.317_{\pm 0.019}$	147	$0.314_{\pm 0.021}$	421	$0.323_{\pm 0.014}$	35	$0.300_{\pm 0.044}$
4	420	483	$0.331_{\pm 0.023}$	131	$0.322_{\pm 0.024}$	329	$0.330_{\pm 0.017}$	23	$0.389_{\pm 0.059}$
tot	-	1319	$0.347_{\pm 0.029}$	336	$0.336_{\pm 0.028}$	913	$0.349_{\pm 0.019}$	70	$0.365_{\pm 0.081}$
E^i_{pk}		250		256		249		241	

	total			genuine short		
sp	N_{grb}	E^i_{pk}	$\langle V/V_{max}\rangle$	N_{grb}	E^i_{pk}	$\langle V/V_{max}\rangle$
1	228	65	$0.450_{\pm 0.019}$	58	65	$0.423_{\pm 0.033}$
2	185	120	$0.395_{\pm 0.021}$	52	122	$0.387_{\pm 0.037}$
3	207	175	$0.296_{\pm 0.018}$	43	176	$0.267_{\pm 0.038}$
4	216	250	$0.283_{\pm 0.018}$	52	255	$0.279_{\pm 0.035}$
5	483	420	$0.326_{\pm 0.013}$	131	420	$0.322_{\pm 0.024}$
tot	1319	250	$0.345_{\pm 0.017}$	336	256	$0.336_{\pm 0.032}$
	long duration			disguised short		
1	163	67	$0.456_{\pm 0.023}$	12	60	$0.511_{\pm 0.095}$
2	116	119	$0.402_{\pm 0.027}$	15	122	$0.293_{\pm 0.062}$
3	154	172	$0.295_{\pm 0.021}$	9	183	$0.321_{\pm 0.092}$
4	151	249	$0.291_{\pm 0.023}$	11	265	$0.294_{\pm 0.089}$
5	329	420	$0.330_{\pm 0.017}$	23	420	$0.309_{\pm 0.059}$
tot	913	249	$0.349_{\pm 0.021}$	70	241	$0.339_{\pm 0.076}$

GRB rate density

Wanderman & Piran (2011MNRAS..406..3..1944) obtains an expression with similar shape of Schmidt (2009), as

$$GR^{ob}_{WP}(z) = \begin{cases} (1+z)^{n_1} & \text{if} \quad z \leq z_1 \\ (1+z_1)^{n_1-n_2}(1+z)^{n_2} & \text{if} \quad z > z_1 \end{cases}, \qquad (3)$$

where the parameter n_1, n_2 and z_1 are adjusted according to the observations, thus Wanderman & Piran yields $z_1 = 3.1^{+0.6}_{-0.8}$, $n_1 = 2.1^{+0.5}_{-0.6}$ and $n_2 = -1.4^{+2.4}_{-1.0}$.

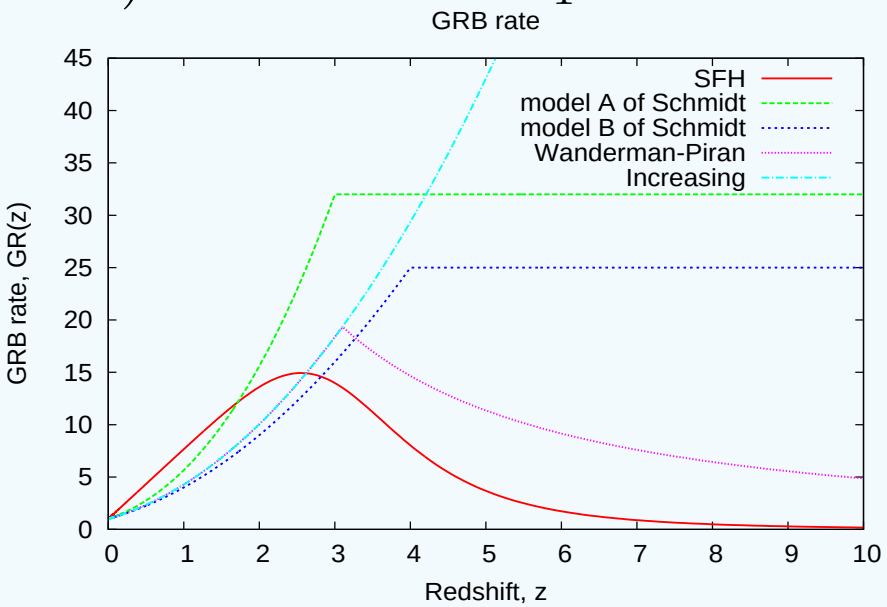

K-correction

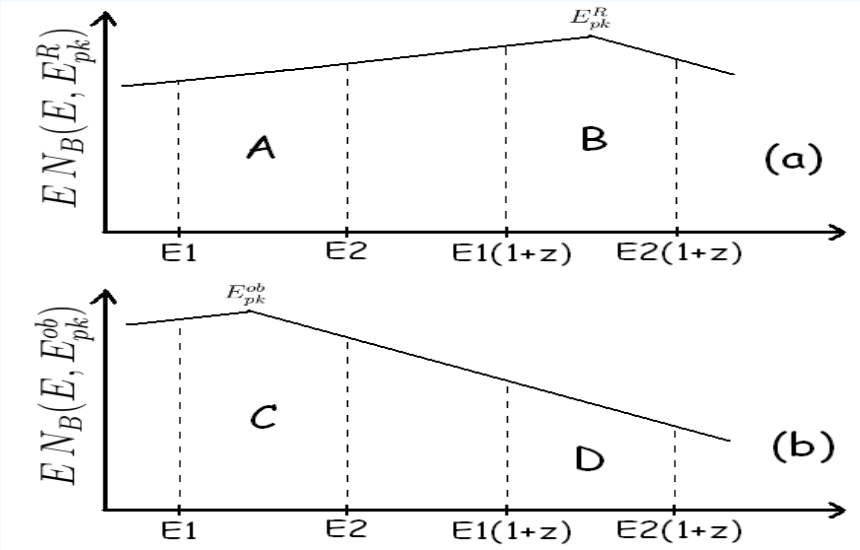

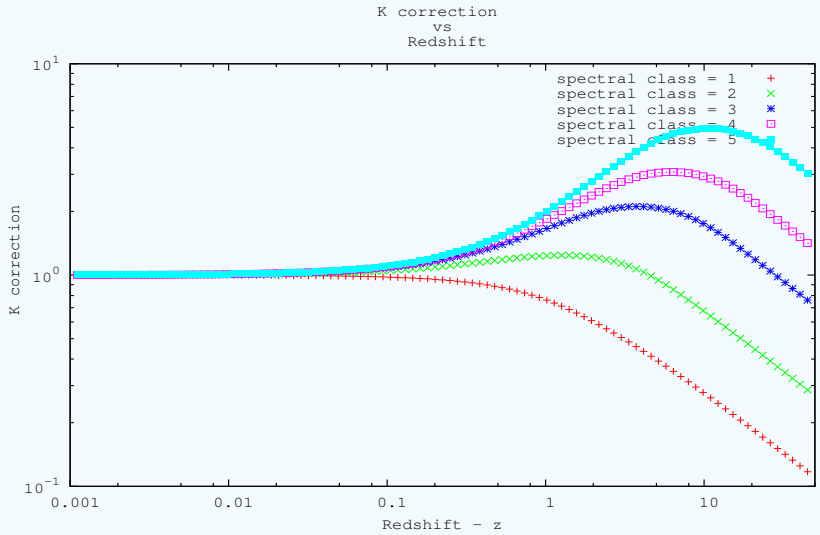

The K-correction is defined by

$$F^{en}_{pk} = \frac{L^R_{pk} k(z)}{4\pi [D_L(z)]^2}, \qquad k(z) = \frac{\int_{E_1(1+z)}^{E_2(1+z)} E\, N_B(E, E^{ob}_{pk}) dE}{\int_{E_1}^{E_2} E\, N_B(E, E^R_{pk}) dE},$$

where $N_B(E, E_{pk})$ is the Band function.

Luminosity function

Luminosity function is given by

$$\Phi(L, z, sp) = \Phi_0(L, sp) GR(z),$$

$$\Phi_0(L, sp) \propto \exp\left\{ - \left[\log\left(\frac{L}{L_c(sp)} \right) \right]^2 \right\}$$

where Φ_0 is the LF of GRBs at $z = 0$.

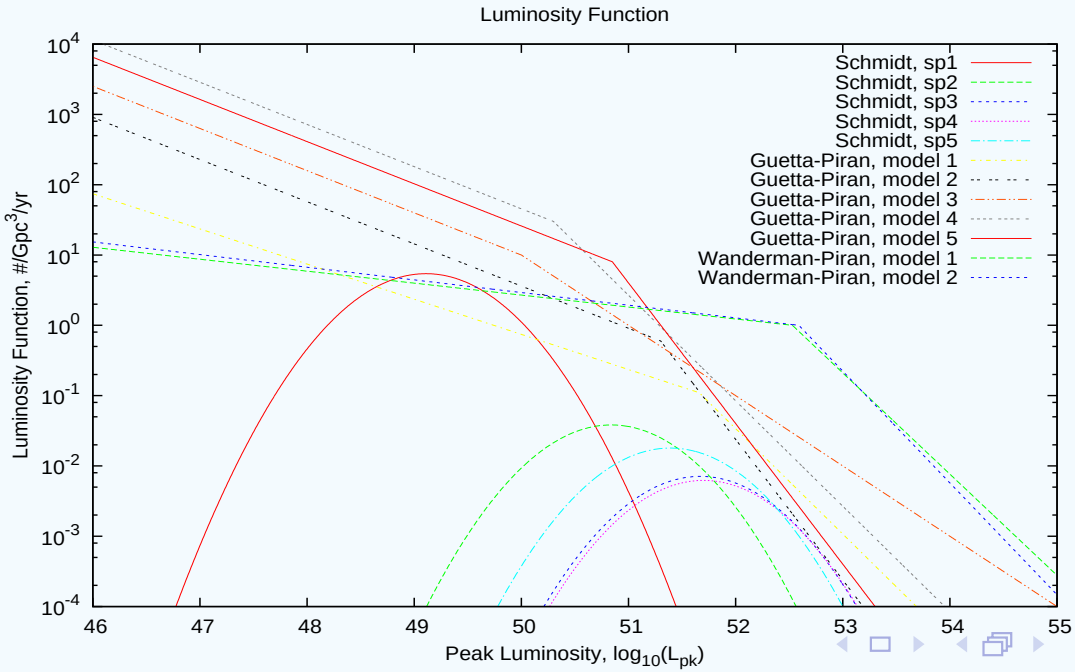

Source count

We obtain the source count integrating the luminosity function

$$N(F > F_{lim}, sp) = \int_0^\infty \phi_0(L, sp) dL \int_0^{z(L,F,sp)} \xi(z') dz', \quad (4)$$

$$N(L, sp) = \phi_0(L, sp) \int_0^{z(L,F_{lim},sp)} \xi(z') dz', \quad (5)$$

$$N(z, sp) = \xi(z) \int_{L(z,F_{lim},sp)}^\infty \phi_0(L', sp) dL', \quad (6)$$

where

$$\xi(z) = GR^{com}(z) \frac{dV_{com}}{dz} = 4\pi \frac{GR^{ob}(z)}{1+z} [D_{com}(z)]^2 \frac{dD_{com}(z)}{dz}.$$

where $D_{com}(z)$ is the comoving distance and $GR^{com}(z) = GR^{ob}(z)/(1+z)$ and $GR^{ob}(z)$ are the intrinsic GRB rate density in, respectively, comoving and observer frames.

Table of sources with known redshift

GRB name	redshift	Δt	t_{pk}	E_{pk}^{ob}	$\log_{10}(L_{iso})$	F_{pk}^{ph}	detector
111008A	4.9898	250	10	149.00	52.17	3.41	1
110801A	1.858	580	370	140.00	50.64	0.57	1
110731A	2.83	7.3	0.13	304.00	52.41	20.9	2
110715A	0.82	20	2	148.00	51.66	35.63	3
110503A	1.613	12	2.3	211.00	52.19	31.27	3
110422A	1.77	40	18	246.00	52.26	31.74	3
110213B	1.083	75	20	123.00	50.78	2.41	3
110213A	1.46	35	21	98.40	51.97	17.7	2
110205A	2.22	330	210	222.00	51.10	1.42	3
110128A	2.339	12	6	–	51.12	1.6	2
110106B	0.618	52.2	42.7	–	50.23	2.77	2
101219B	0.5519	51	9.7	70.00	50.04	2	2
101219A	0.718	0.6	0.03	426.00	51.65	54.17	3
100906A	1.727	150	9.7	180.00	51.69	8.19	3
100901A	1.408	495	3.2	–	50.29	0.6	1
100816A	0.8034	8.45	0.9	148.00	50.96	7.45	3
100814A	1.44	156	1	147.00	51.03	2.43	3
100728B	2.106	6.6	2.2	104.00	51.85	6.2	2
100724A	1.288	4	0.1	–	50.59	1.42	1
100621A	0.542	74	26.9	83.00	50.50	6.07	3
100518A	4	42	4	–	50.86	0.37	4
100513A	4.772	100	41.09	–	51.05	0.45	1
100425A	1.755	110	45.27	–	50.71	1.05	1
100418A	0.6235	50	10.47	–	49.67	0.75	1
100414A	1.368	26.4	20.5	595.00	51.71	16.78	3
100316D	0.059	64	80	–	46.52	0.07	1
100316B	1.18	20.4	0.3	–	50.35	0.97	1
100302A	4.813	30	23.87	–	50.98	0.37	1
100219A	4.6667	60	41.89	–	50.86	0.3	1
100117A	0.92	0.4	0.35	287.00	50.95	6.1	2
091208B	1.063	19.5	8.35	144.20	51.25	7.71	1
091127	0.49	8.45	0.14	130.00	50.92	20.8	1
091109A	3.076	55	23.2	–	51.10	0.97	1
091029	2.752	61.97	20.89	61.22	51.18	0.55	1
091024	1.092	150.18	15.96	–	50.49	1.56	1
091020	1.71	56.74	9.62	47.90	51.07	1.12	1
091018	0.971	8.02	1.07	19.43	50.63	1.47	1

Results - CONFRONTING SUBSAMPLES

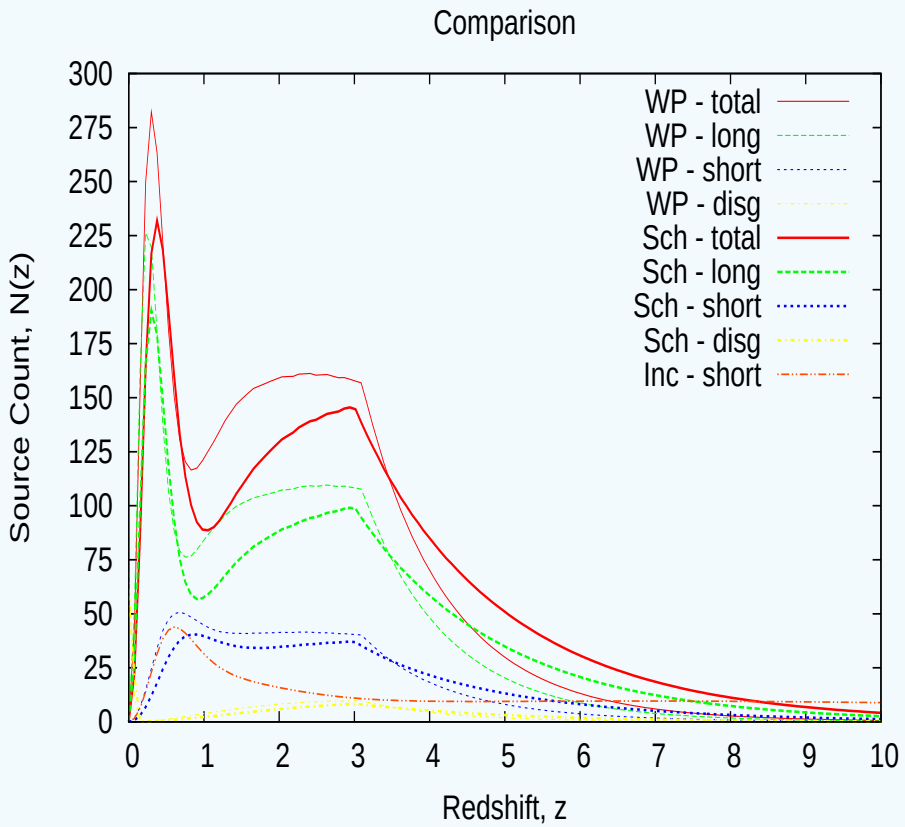

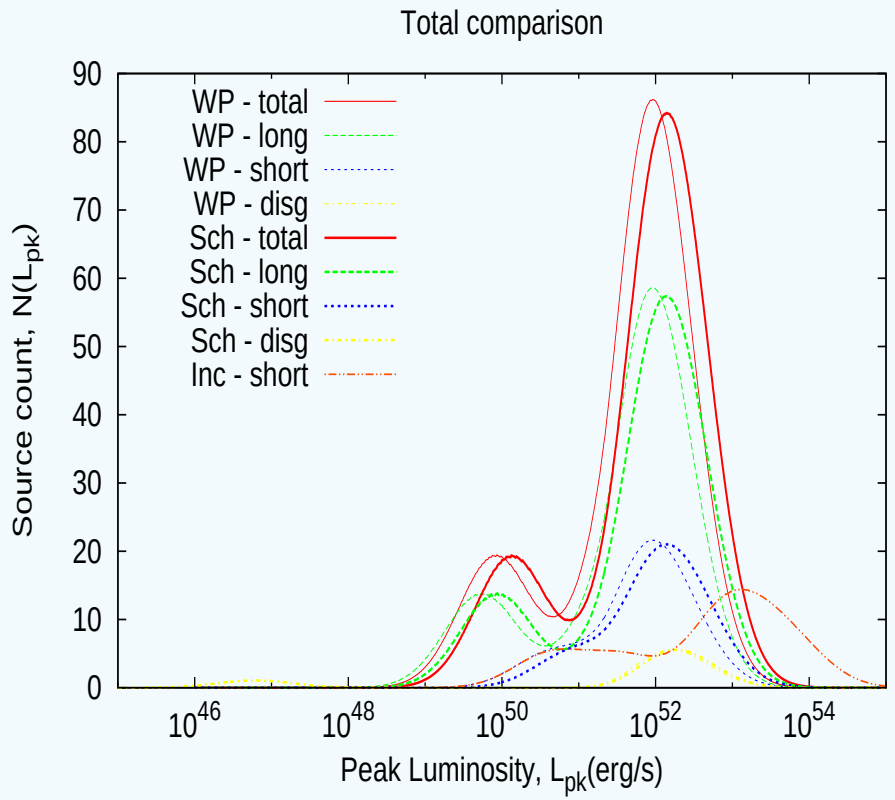

Results - PREDICTED vs OBSERVED

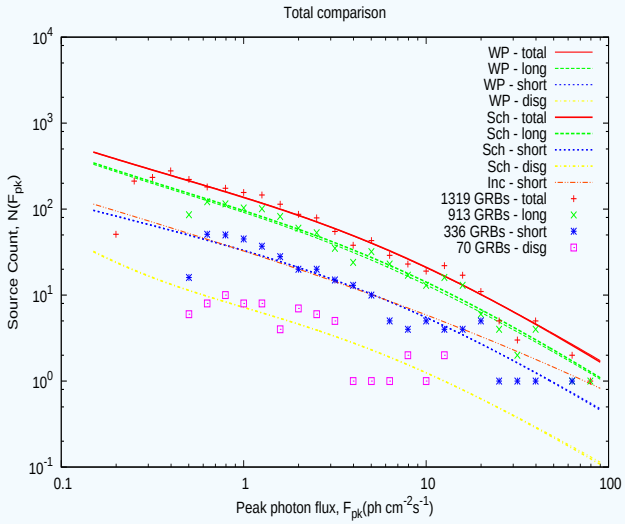

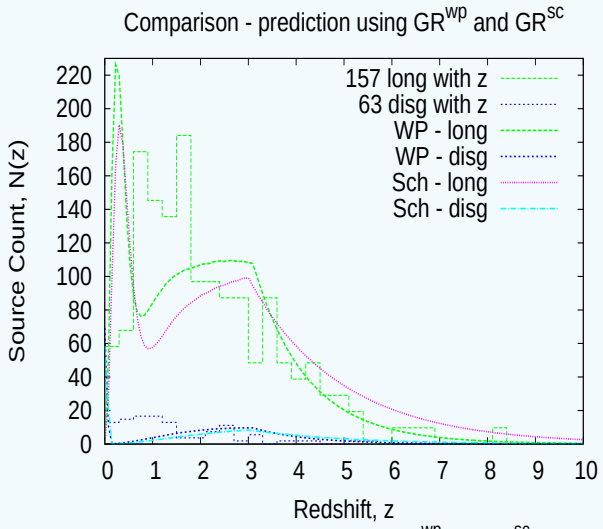

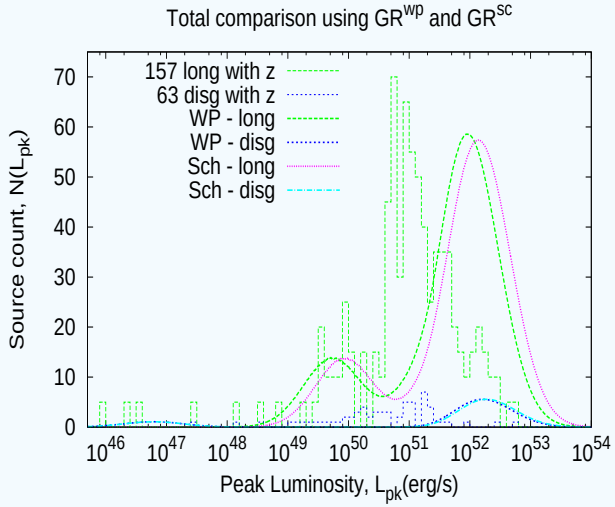

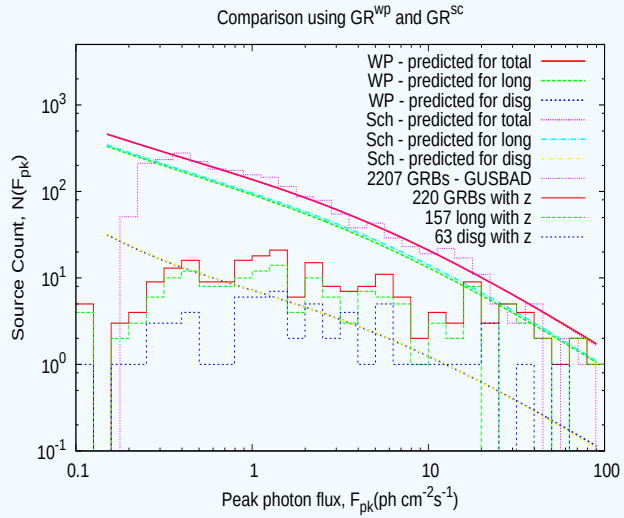

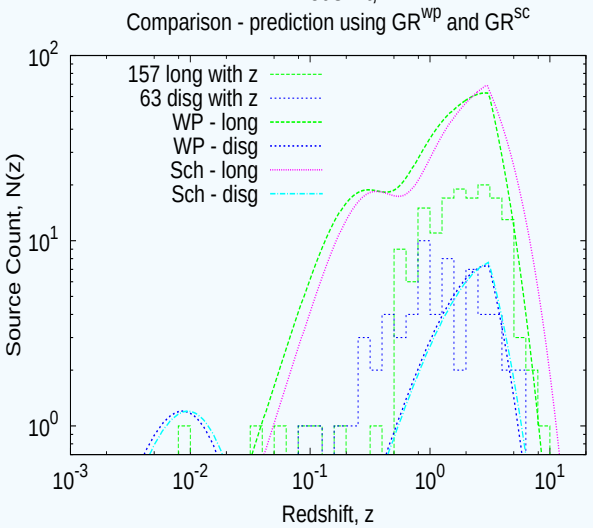

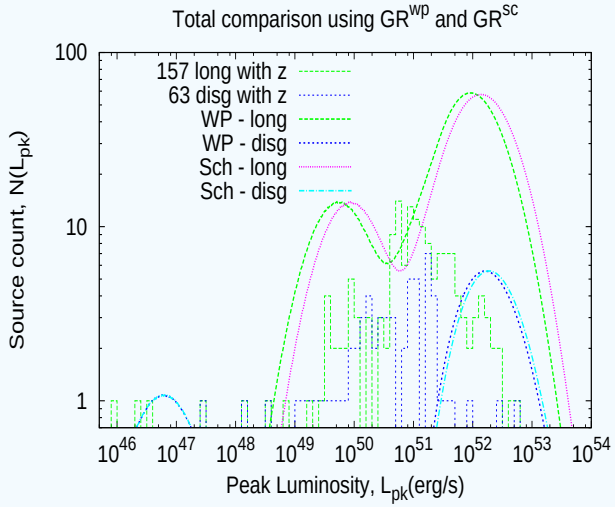

PREDICTED vs OBSERVED

Comparing the predicted (by LF statistic) and the observed (sources with known redshifts) distributions, we obtained that it is not possible to compare, because the sources with known redshift form a peculiar sample, where they are only sources in which we are able to identify the redshift. To perform a honest comparison, it is necessary to built a special GRB rate density for this peculiar sample of sources with known redshift.

Malmquist bias

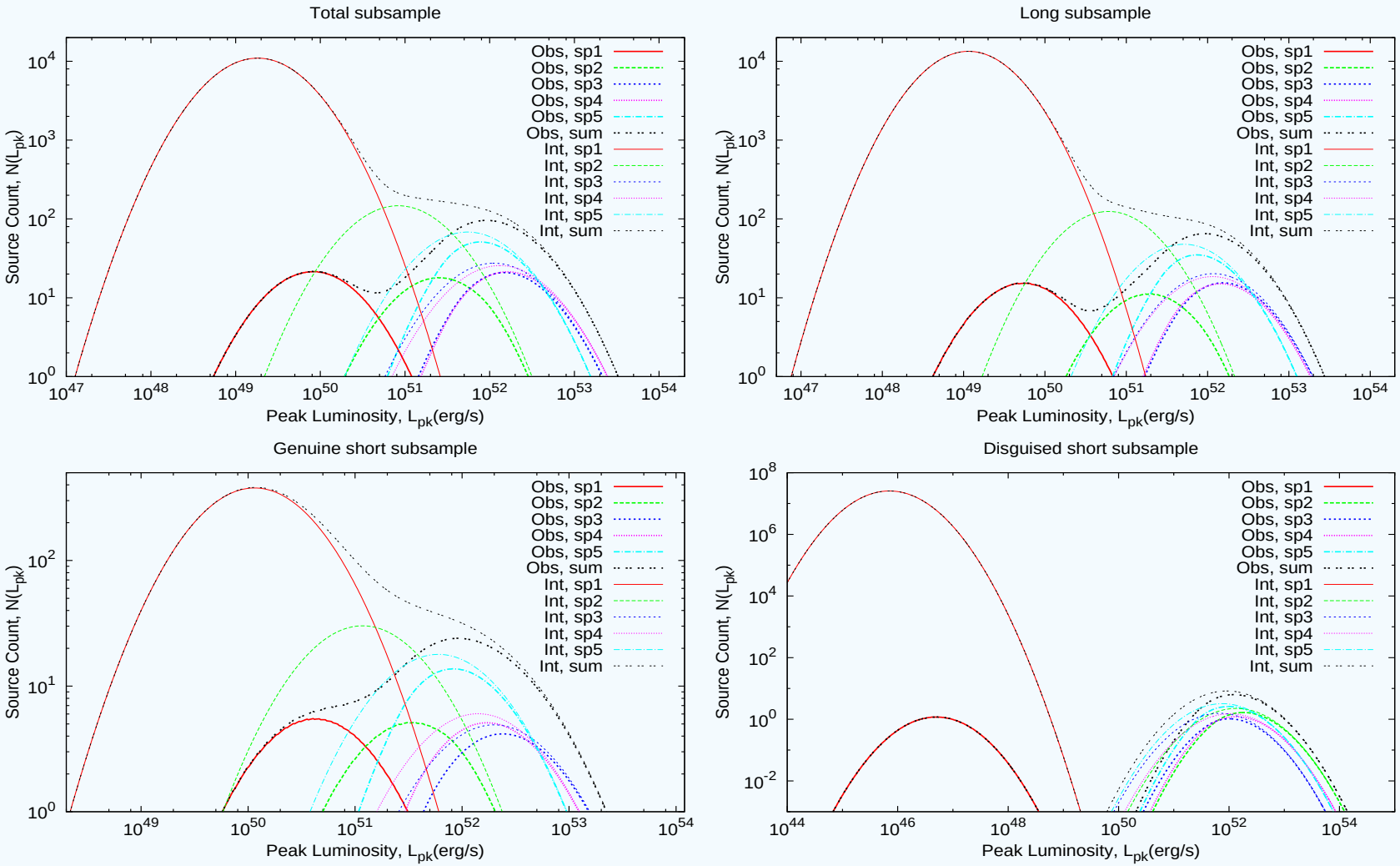

L_{iso} vs E_{pk} correlation

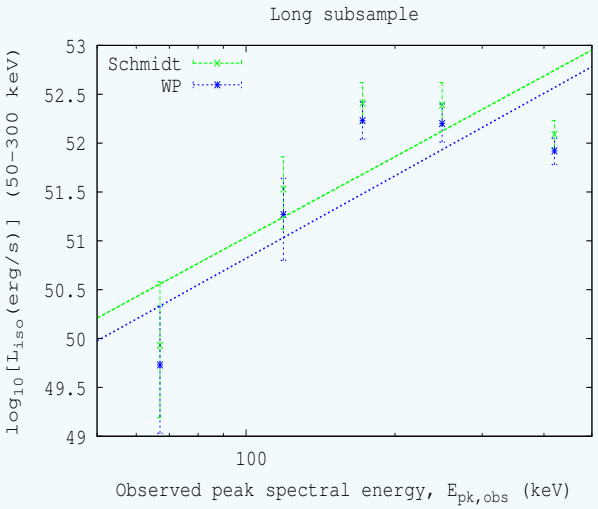

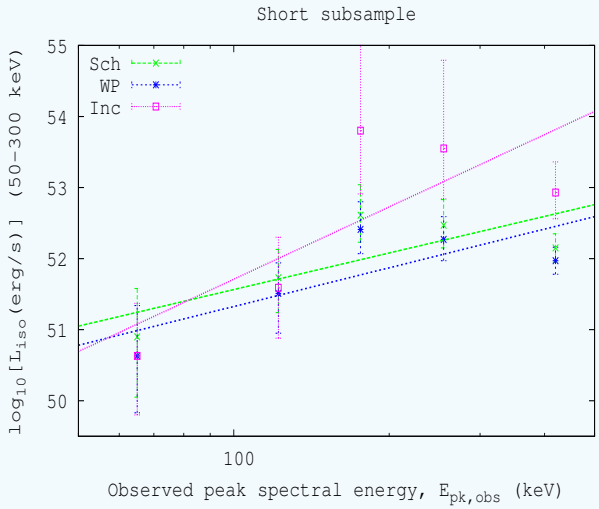

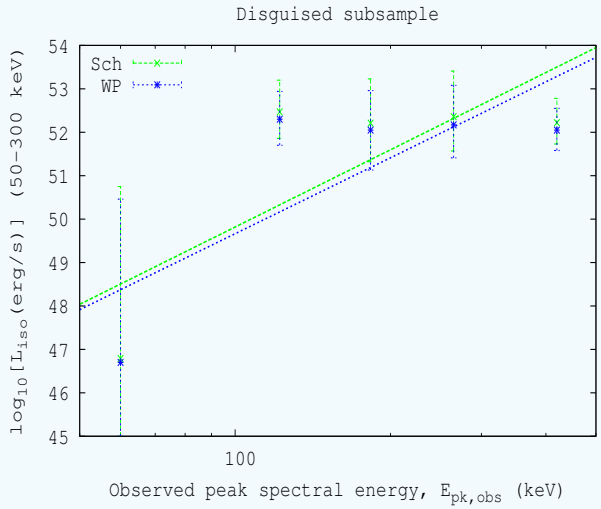

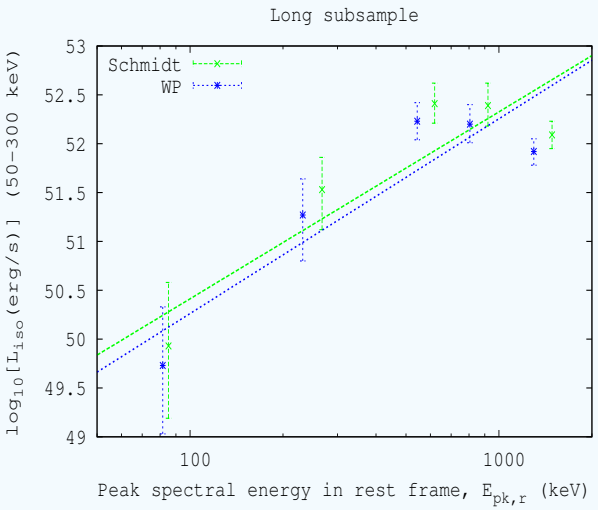

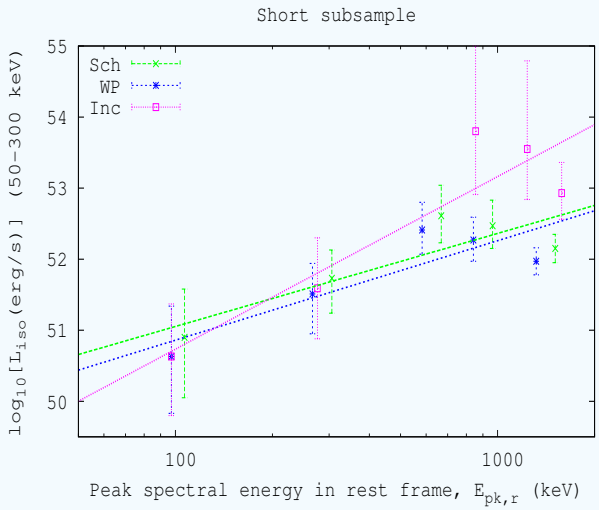

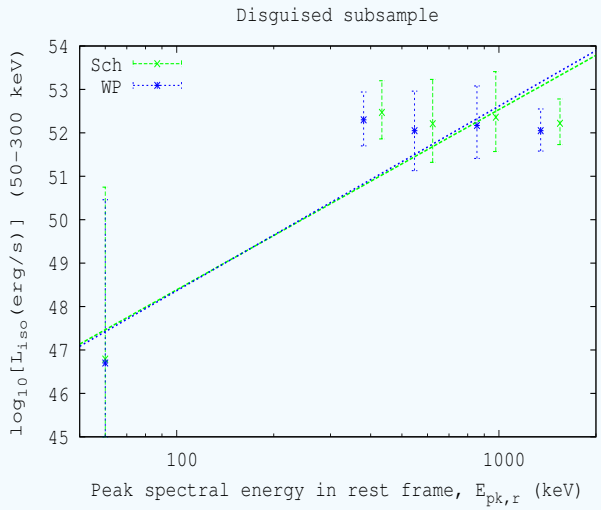

L_{iso} vs E_{pk} correlation

Both figures show the Hertzsprung-Russell diagram.

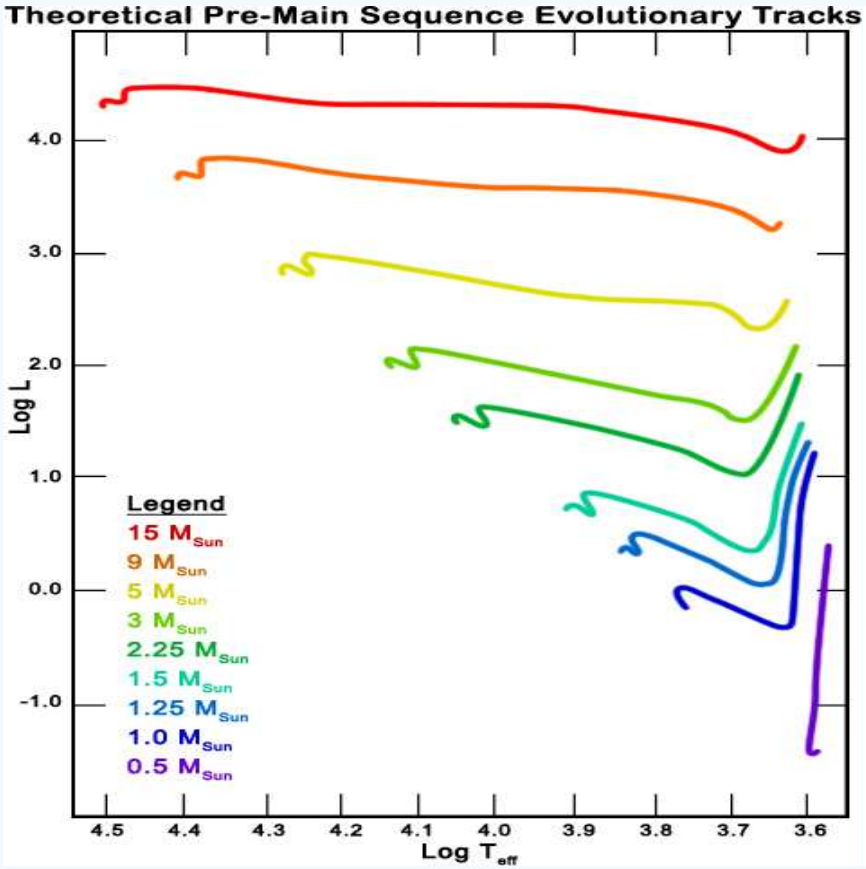

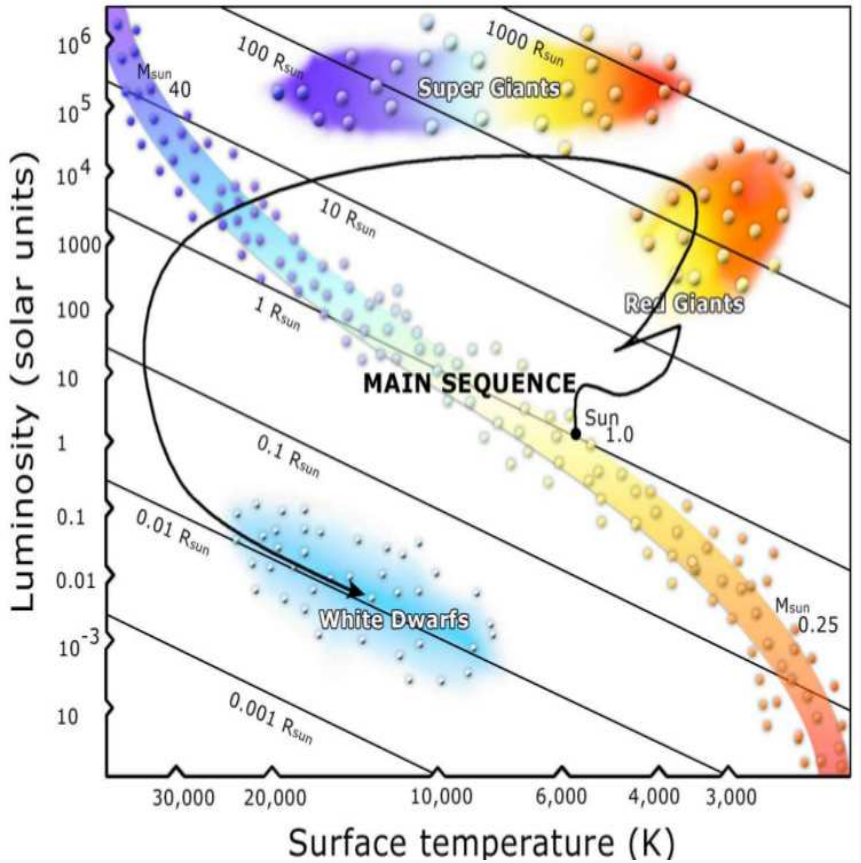

Conclusions1

- In the application of the LF statistics we confirmed the prediction by the *Fireshell model* about the existence of three GRB classes (*long duration*, *genuine short* and *disguised short*).
- We built a table with data of 220 GRBs with known redshift, data obtained from six different detectors. We noted that it is not possible compare with the distribution of the sources obtained from this table with the ones obtained from LF statistic, because the sources with known redshift form a particular sample.

Conclusions2

- We estimated the effects of the Malmquist bias for the subsamples predicted by the Fireshell model.
- We looked for a correlation like $L_{iso} - E_{pk}$ (like Amati or Ghirlanda relation) through the LF statistic for the four subsamples, but we believe that it is unlikely that there is a correlation like power law using the BATSE data.

THANKS